ISSN (Print) 1226-1750
ISSN (Online) 2233-6656
Journal of Magnetics 25(3), 347-354 (2020) https://doi.org/10.4283/JMAG.2020.25.3.347

Influence of Laminating Materials and Modified Pole Shapes on the Performance of Segmented Rotor Switched Reluctance Motor

Augustine Mathu Gnaniah[1]*, Balaji Mahadevan[2], and Kamaraj Vijayarajan[3]

[1]*Deparment of Electrical and Electronics Engineering, Loyola-ICAM College of Engineering and Technology, Chennai, India*
[2]*Deparment of Electrical and Electronics Engineering, SSN College of Engineering, Chennai, India*
[3]*Deparment of Electrical and Electronics Engineering, SSN College of Engineering, Chennai, India*

(Received 15 April 2020, Received in final form 13 July 2020, Accepted 1 September 2020)

This work deals with the torque ripple minimization techniques of Segmented Rotor Switched Reluctance Motor (SSRM) for cooling fan application. Torque ripple, acoustic noise and vibration are factors resisting the segmented rotor SRM. To overcome this, stator and rotor pole modifications along with the effects of laminating steel material have been analyzed for the performance improvement of the machine. The performance of the machine with different laminating steel materials such as M19, M850-65A, M890-50d and M43 are compared with the conventional CR-10 steel material. With respect to pole shape modifications the analysis has been performed by considering stator pole taper, stator pole arc, rotor segement structure and rotor pole depth. The results highlight the influence of structural modifications and material properties on the performance of the motor. The results of electromagnetic analysis disclose that the segmented rotor configuration with M890-50d material exhibits superior electromagnetic characteristics.

Key words : Switched Reluctance Motor (SRM), segmented rotor, electromagnetic analysis, M850-65A, M43, M890-50d, Cold Roll Silicon Steel (CRS)

1. Introduction

The research on the application of Switched Reluctance Motor (SRM) for industrial and domestic is on the upswing [1]. However, the enrichment in the torque density and efficiency of the SRM continues to be the major concern [2]. In order to reduce the acoustic noise and to improve the efficiency, novel SRM configurations with flux reversal free stator has been urged [4]. The effect of the magnetization behaviour of the different core materials has been illustrated in [8, 9] for enhancing the performance of the machine.

The number of stator poles and rotor segments selection manner has been reviewed by Vandhana *et al.* [2]. The performance enhancement of SRM due to the impact of core material has been revealed in [7]. The performance evaluation of SRM due to the influence of pole arc has been figured out in [10]. A new design of rotor segment parameters which reduces the torque ripple has been proposed in detail by Iqbal Hussain [19]. The sensitivity of geometrical parameters on the performance of SRM has been described in [10-15]. In [15], in order to finalize the modified pole shape configuration, the sensitivity of the stator and rotor pole arcs has been analyzed to minimize torque ripple.

From the literature, it is imperative that analysis of SSRM combined with different pole shape modifications and different material properties provides splendid opportunities to explore and scale up the application prospects of SSRM. In this perspective, this work researches various design configurations on stator as well as rotor side to analyse the performance of the SSRM. Hence, different geometrical parameters and laminating materials have been considered and an in-depth electromagnetic analysis has been pursued. To emphasize the merits of proposed design modifications and material properties, a comparison has been drawn with respect to conventional 6/5 SSSRM structure. The results have been illustrated with respect to a 500 W cooling fan motor. By using the Finite Element Analysis (FEA)-based Computer Aided Design (CAD) package the performance measures have been investigated.

*Corresponding author: Tel: +91-9790395731
Fax: +91-462-2352961, e-mail: gnanaugus@gmail.com

2. 6/5 Flux Reversal Free Segmented Rotor SRM

A flux reversal free structure for 6/5 configuration is shown in Fig. 1. The E-core structure of stator enables the flux reversal free operation [16].

Due to the segmented and E-core configuration, the utilization of electrical energy has been improved and the MMF requirements have also been reduced [13, 6]. The configuration has six stator poles with main as well as auxiliary poles. The main pole contributes to flux production and the auxiliary poles are used for the reversal of flux in the stator core. The rotor is a segmented rotor configuration in which laminated steel materials are embedded in the non-magnetic aluminium core. As a result, electric utilization has been improved.

The flux path of the proposed Segmented Rotor SRM through FEA analysis is shown in Fig. 2, 3 & 4 for each phase excitation, in which the flux reversal free concept is revealed.

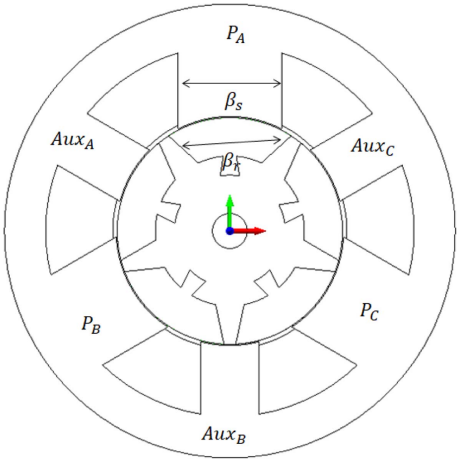

Fig. 1. 6/5 SSRM with flux reversal free structure.

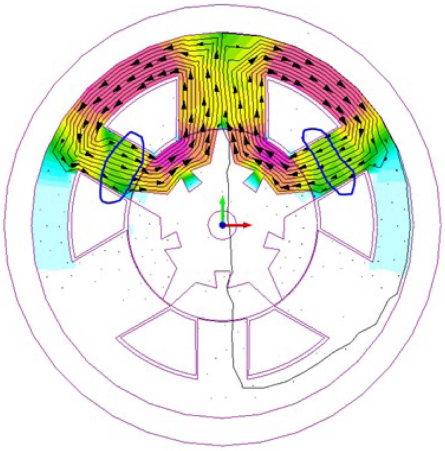

Fig. 2. Flux path for phase-A excitation.

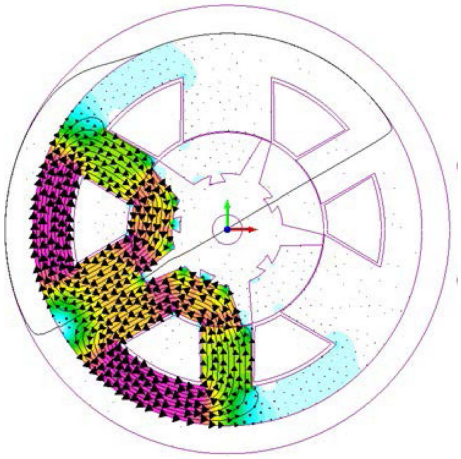

Fig. 3. Flux path for phase-B excitation.

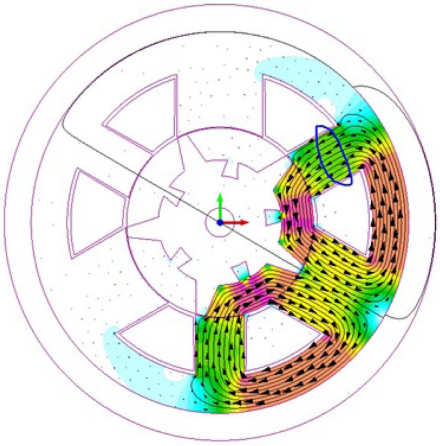

Fig. 4. Flux paths for phase-C excitation.

The performance analyses of the Segmented Rotor Switched Reluctance Motor (SSRM) compared to conventional and 12/8 segmented configurations are tabulated in Table 1.

The result reveals poor torque ripple for the segmented rotor SRM. In order to reduce the torque ripple, geometrical modifications and new laminating materials have been analysed.

Table 1. Torque Ripple and Total Losses for Different Configurations.

Model	Torque Ripple (p.u)	Total Losses (Watts)
Conventional 12/8 SRM	1.504	111.25
12/8 Segmented Rotor SRM	2.126	36.27
6/5 Segmented Rotor SRM with E-core	1.891	28.42

3. Analysis with Different Lamination Materials

In switched reluctance motor, the loss component includes core losses as well as ohmic losses. Since there is no winding in the rotor, SRM generates less ohmic losses. But in the performance evaluation, the effect of core losses plays a key role. Flux density and permeability of material are the major components which contribute to the core loss in the reluctance motor [4]. Hence the selection of material plays a vital role in influencing the performance of the machine. In this perspective this paper explores different materials like M-19, M800-65A, M-43 and M890-50D for the performance enhancement of SSRM. The corresponding BH curve comparison for different laminating materials considered in this work is shown in the Fig. 5.

The structure of 6/5 SSRM with M890-50D material is shown in Fig. 6.

The corresponding core loss of the SSRM can be calculated as follows.

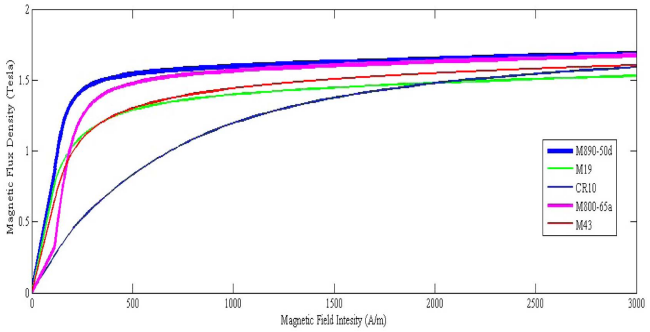

Fig. 5. BH comparison for different Laminating Material.

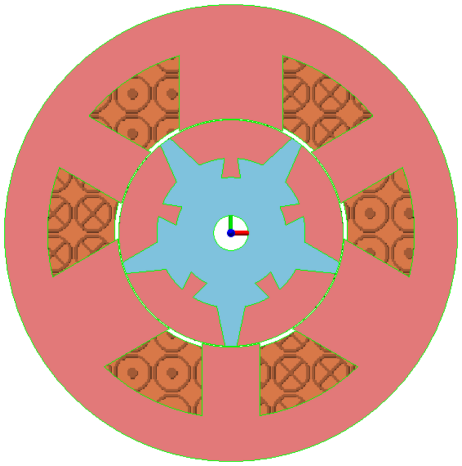

Fig. 6. Structure of 6/5 SSRM with M890-50D Laminating Material.

Table 2. Core Loss Coefficients for Laminating Materials.

Laminating Material	K_h (W/kg)	K_e (W/kg)
M-19	0.02703	$0.5e^{-6}$
M-43	0.0566	$0.1e^{-6}$
M800-65A	0.0632	$2.58e^{-5}$
M890-50D	0.051793	$0.13e^{-6}$

$$W_c = W_h + W_e \tag{1}$$

Where W_c – Total Core loss, W_h – hysteresis loss, W_e – eddy current loss.

The hysteresis loss can be calculated from

$$W_h = K_h f B_m^2 \tag{2}$$

Where K_h – hysteresis loss coefficient, B_m – maximum flux density

The eddy current losses can be calculated from

$$W_e = K_e f^2 B_m^{1.5} \tag{3}$$

Where K_e – eddy current loss coefficient, $B_m{}^{1.5}$ – maximum flux density with Steinmetz exponent value

The corresponding core loss coefficient values of different

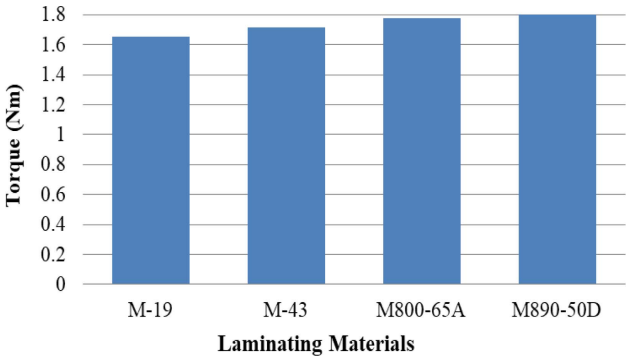

Fig. 7. Average Torque Profile for Different Laminating Materials.

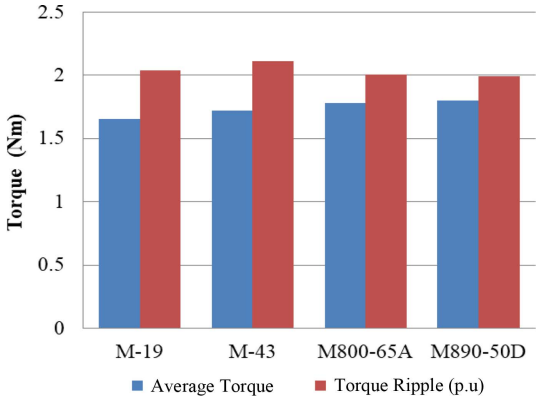

Fig. 8. Comparison of Torque Ripple and Average Torque for Different Laminating Material.

Table 3. Core Losses and Total Losses for Different Laminating Materials.

Material	Iron Losses (Watts)	Losses (Watts)
CR-10	22.12	28.42
M-19	19.55	24.76
M-43	16.67	21.90
M800-65A	36.31	41.53
M890-50D	15.80	21.02

materials are tabulated in Table 2.

In this perspective, the electromagnetic analysis has been carried out for different materials under static and dynamic conditions. The calculated average torque values for different laminating materials are shown in Fig. 7. The variations in torque ripple and torque average for the different laminating materials are shown in Fig. 8.

The core loss and total loss values for different laminations are tabulated in Table 3. From the results, it has been observed that M890-50D has better performance compared to other laminating materials.

4. Analysis with Rotor Pole Modification

Segmented rotor configuration in SRM makes a huge difference between the conventional and proposed in terms of average torque and power density. Since the SSRM has flux reversal free stator, the flux leakage will be reduced in order to increase the power density as well as the utilization of flux. The SSRM exhibits superior performance than the conventional SRM [16]. One of the major drawbacks of the SSRM is torque ripple. In order to reduce the torque ripple, various geometrical design modification techniques have been introduced in this paper.

4.1. Selection of Rotor Segment Structure

The design specification is normally based on the inductance profile of the SSRM because the inductance profile gives the appropriate position to switch the phase windings. By introducing a dip in the center of the rotor structure, the inductance profile has been varied [19]. In this paper, rotor structure with dip and curved structures are introduced. Furthermore, electromagnetic analysis was carried out to identify the superior design which would provide lower torque ripple for 6/5 SSRM machine. The torque ripple can be calculated using the formula:

$$T_{ripple} = \frac{T_{\max} - T_{\min}}{T_{avg}} \quad (4)$$

Five different segmented structures are considered for the analysis. The initial design is considered as a conventional rotor structure which promotes better performance compared with the other variations. Design 2 of SSRM is framed by introducing fillets in both the edges of the segmented pole. Design 3 and 4 are constructed by introducing dip in the center. Design 5 is constructed by introducing fillet in the one end of the rotor pole. Lastly, design 6 is constructed with dip, fillet and normal design the various structures are shown in the Fig. 9.

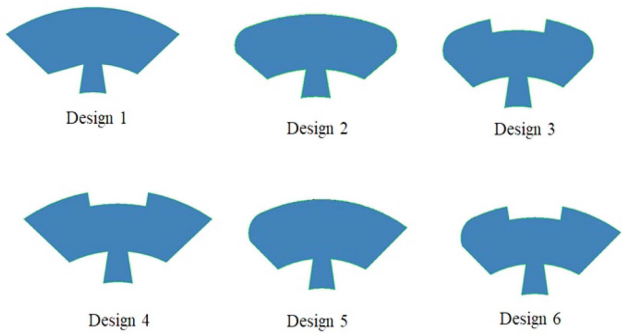

Fig. 9. Different Rotor Segment Structure.

Table 4. Performance Comparison for Different Rotor Structure.

Design	Average Torque (Nm)	Torque Ripple (p.u)	Losses (Watts)
1	1.65	2.038	24.76
2	1.41	2.666	13.67
3	1.29	2.610	14.67
4	1.46	1.847	20.84
5	1.53	1.646	15.71
6	1.38	1.781	18.88

The average torque, torque ripple and losses are tabulated in Table 4. The results show that the initial design promotes better performance in comparison with other designs.

4.2. Selection of Rotor Pole Depth

In the torque production process, the role of electromagnetic utilization is vital [3]. The improvement in flux utilization will lead to better performance. The segmented rotor configuration provides effective utilization of flux. But the 6/5 SSRM exhibits poor torque ripple [16]. Hence, pole shape modification is carried out to reduce the torque

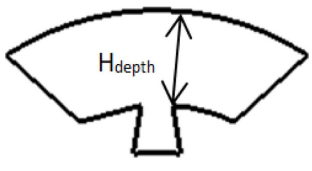

Fig. 10. Rotor pole structure of Segmented Rotor SRM.

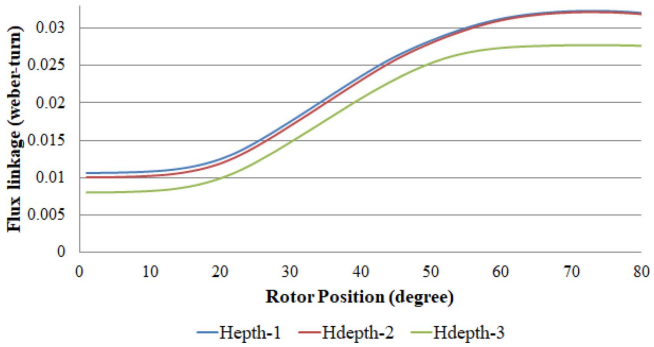

Fig. 11. Flux Linkage Characteristics for different H_{depth}.

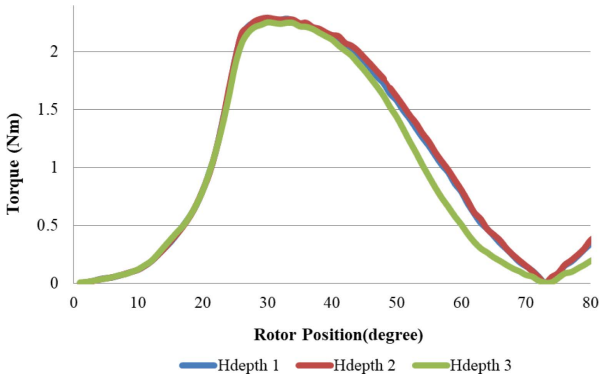

Fig. 12. Static Torque Characteristics for different H_{depth}.

ripple. The various depths (H_{depth}) are considered for torque ripple minimization. The structure of the rotor pole for a segmented rotor SRM is shown in the Fig. 10.

For various geometrical configurations the average torque, ripple and losses are considered for both M-19 material as well as the M890-50D material. The static inductance profile for various depths and the corresponding static torque characteristics are shown in Fig. 11 and 12. From the graph it is evident that the design Hdepth-2 exhibits higher inductance and in turn results in wider torque characteristics resulting in lower torque ripple. The Table 5 and Table 6 illustrates the average torque and torque ripple comparison for different pole depths.

Table 5. Average Torque for Different Pole Depths.

Material	H_{depth}-1	H_{depth}-2	H_{depth}-3	H_{depth}-4
M-19	1.62	1.64	1.65	1.50
M890-50D	1.80	1.83	1.79	1.62

Table 6. Torque Ripple for Different Pole Depths.

Material	H_{depth}-1	H_{depth}-2	H_{depth}-3	H_{depth}-4
M-19	1.6432	1.6013	1.7098	1.7336
M890-50D	1.4329	1.5613	1.9923	1.6648

From the results it is evident that the ripple can be reduced by changing the pole depth hence the optimized pole depth has been considered for further analysis. From this technique the pole depth H_{depth}-2 has been chosen as it reveals better performance compared to other choices

5. Analysis with Stator Pole Modification

5.1. Influence of pole arc on the perfromance of machine

The torque production in the SRM always depends on the flux linkage in the airgap and rotor pole. Also, the electromagnetic torque produced by the machine depends upon the inductance and pole arc value. The electromagnetic torque (T_e) for the SRM machine is given as

$$T_e = \frac{1}{2} k_i i^2 \frac{L_a}{\beta_s} \tag{5}$$

Where K_i – Torque constant, L_a – Inductance at aligned position, β_s – Stator Pole arc.

Since the stator pole arc plays a major role in the torque ripple, different pole arc designs are considered for the torque ripple minimization in this paper, resulting in the torque ripple being reduced for some parameters. The electromagnetic analysis for the different pole arc values are carried out using FEA tool. The FEA analysis carried

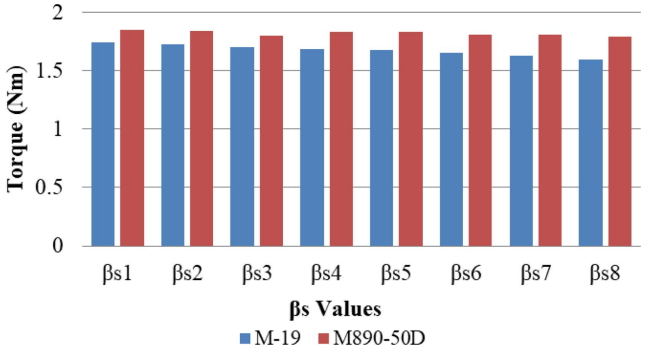

Fig. 13. Average Torque Profile for Different β_s values.

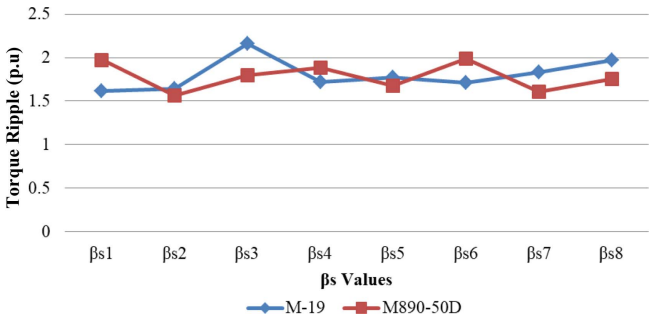

Fig. 14. Torque Ripple Profile for Different β_s values.

out for the same pole arc values on considering the material property as M890-50D. The average torque and torque ripple variations for different design are shown in the Fig. 13 and Fig. 14 correspondingly, for the design '$\beta_s 2$' result reveals better performance on comparing both the torque ripple and average torque values.

5.2. Influence of Tapered Stator Pole

In the flow of torque ripple optimization techniques, tapered stator pole configuration is considered. By tapering the stator pole arc, the slot area of the winding can be controlled. So that the flux density varies,resulting in reduction of torque ripple [11]. The different tapered ratio configurations are considered for the analaysis.Tapered stator pole sturcture is shown in Fig. 15.

Tappered ratio concept can be illustrated by the equation as,

$$\alpha = \frac{\beta_s'}{\beta_s} \tag{6}$$

Where α – Pole arc ratio, β_s' – Modified stator pole arc, β_s – Existing stator pole arc.

Here the value of β_s will be maintained constantly and the corresponding α values are varied from 0.5 to 1.2. The correponding performance values are compared and shown in the Fig. 16. and Fig. 17. for the proposed laminating material M890-50D. The results reveals that the torque ripple has been reduced sufficiently. On considering the

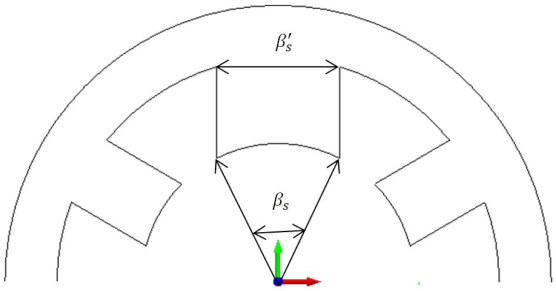

Fig. 15. Structure of Tappered Stator Pole.

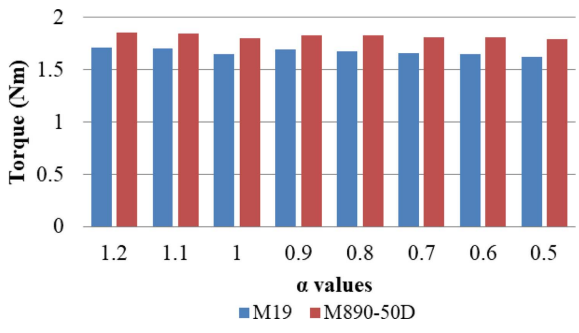

Fig. 16. Average Torque Profile for Different α values.

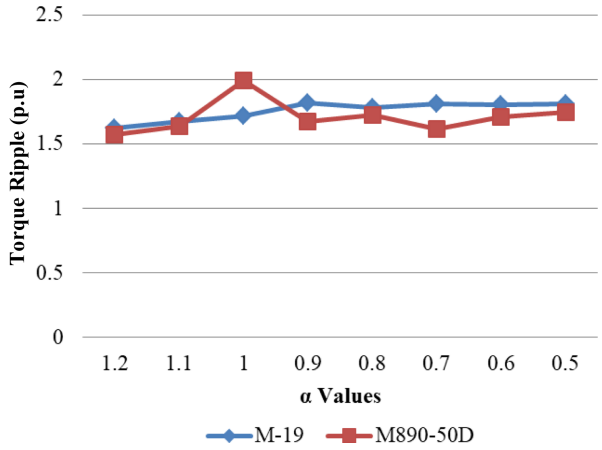

Fig. 17. Torque Ripple Profile for Different α values.

slot area and required average torque it is evident that the design with α value of 0.9 exhibits better performance.

6. Comparative Analysis of Pole Shape Modification and Material Property

After various modification techniques, the final values have been chosen for further electromagnetic analysis, in which the design values of rotor pole depth, stator pole arc and stator tapered values that yields best results are considered. Finally, a novel design which produces low torque ripple has been proposed. The proposed design is compared with M890-50D material. The parameters from various modification techniques considered for further analysis are tabulated in Table 7.

The electromagnetic analysis with the design considering the above parameters has been performed and the analysis illustrated in Table 8 explicates the effects of design modification on average torque. The Table 9 reveals the reduction in the torque ripple which tends to improve the overall performance of the machine. The torque pro-

Table 7. Choice of Design Parameter for the Proposed SSRM.

Description	Values
Rotor Structure	Design-1
Rotor Pole depth	$H_{depth\text{-}2}$
Stator Pole arc	β_{s2}
Tapered stator pole arc	$\alpha = 0.9$

Table 8. Comparison of Average Torque.

Average Torque	CR-10	M-19	M890-50D
Initial Design	1.60	1.65	1.80
Proposed Design	1.71	1.73	1.85

Table 9. Comparison of Torque Ripple.

Torque Ripple	CR-10	M-19	M890-50D
Initial Design	2.124	2.038	1.992
Proposed Design	1.577	1.565	1.525

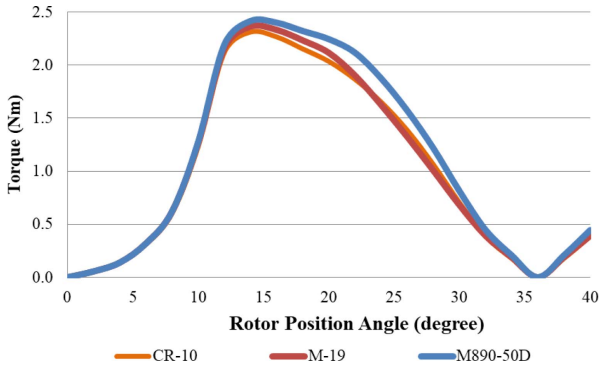

Fig. 18. Torque Profile of 6/5 Proposed SSRM.

file the above best design with different laminating material is shown in Fig. 18. The results reveal that the structure incorporating the design modification with laminating material M890-50D exhibits better performance characteristics.

7. Experimental Validation

The prototype model of proposed SSRM with flux reversal free stator has been fabricated. The fabricated stator and rotor structures are shown in Fig. 19 and Fig. 20, respectively. The results of FEA are validated by experimentally measuring inductance at aligned and unaligned position as detailed in [22]. The area enclosed between the curves flux linkage vs. current for unaligned and aligned positions of the rotor poles with a set of stator poles gives the maximum work done for one stroke of the

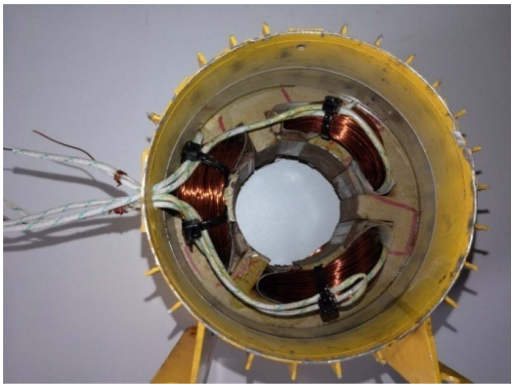

Fig. 19. Stator Components of 6/5 SSRM with E-core Structure.

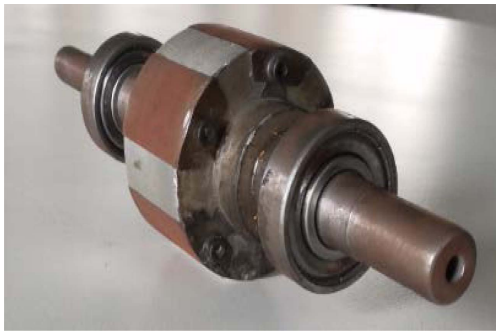

Fig. 20. Rotor Components of 6/5 SSRM.

Table 10. Inductance Comparison.

Model	Aligned Inductance (mH)	Unaligned Inductance (mH)
FEA	0.7826	0.2125
Protoype	0.7982	0.2167

motor. From the fundamental voltage equation the magnetic characteristics of the machine can be determined by applying voltage pulse to any one phase of the machine. The inductance value obtained from FEA during aligned and unaligned positions are tabulated in Table 10. The table depicts the values obtained using experiments correlated to the simulated FEA results. The Comparison of static torque characteristics between the prototype and FEA is illustrated in the Fig. 21. The closeness of the inductance values and static torque characteristics validates

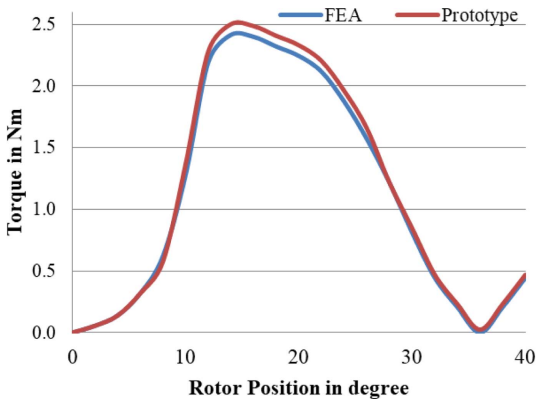

Fig. 21. Torque profile for FEA and Prototype of SSRM.

Table 11. Comparision of Average Torque and Torque Ripple.

Model	Average Torque (Nm)	Torque Ripple (p.u)
Conventional 12/8 SRM	1.65	1.518
Conventional 6/5 SSRM	1.75	2.164
Proposed 6/5 SSRM	1.84	1.546

the analysis.

An overall comparision with respect to different SRM configurations is illustrated in Table 11. The results reveal that in comparsion with the conventional SRM and 6/5 SSRM the configurations with the design modifcations proposed exhibits better average torque. With respect to torque ripple there is significant improvement with respect to initial 6/5 while the conventional SRM outperforms the proposed configuration marginally.

8. Conclusion

In this work, a performance investigation is conducted for a segmented rotor SRM and comparison with different laminating steel material is analyzed. The results are presented with respect to a 500 W motor suitable for cooling fan application. The results indicate that the M890-50D material provides better performance compared to other laminating steel materials. With respect to geometrical modifications, a thorough analysis considering stator pole arc variation, introducing stator pole taper, selection of rotor segment structure and introducing depth in the rotor segments has been performed. A new design is evolved considering the best design values of the above modifications and M890-50D.The results of the design reveal that the 6/5 segmental rotor SRM offers improved efficiency with minimum torque ripple in comparison with conventional SSRM design. Future work will be oriented towards the vibration analysis and thermal analysis of the machine.

Appendix I

Table A. Design Parameters for SSRM.

PARAMETER	Coventional 12/8 SRM	6\5 SRM
Rated Voltage (V)	12	12
Rated Torque (Nm)	1.7	1.7
Rated Speed (rpm)	2800	2800
Number of Phases	3	3
Outer Radius (mm) (R)	52.5	52.5
Yoke Thicknes of Stator (mm) (C)	5	10
Outer Radius of Rotor (mm) (Rr)	31	26
Length of Airgap (mm)	0.25	0.25
Inner Radius of Rotor (mm) (Ri)	24	-
Radius of Shaft (mm)	4	4
Length of Stack (mm)	35	35
Stator Tooth Width (mm)	7.6	20.5/10.5

References

[1] Z. Xu, D. H. Lee, and J. W. Ahn, in Proceedings of IEEE Industry Applications Society Annual Meeting, Addison, TX (2015).
[2] R. Vandana and B. G. Fernandes, IEEE Trans. Energy Convers. **30**, 11 (2015).
[3] ZhenyaoXu and J. W. Ahn, in Proceedings of International Conference on Electrical Machines and Systems (ICEMS), Busan (2013).
[4] W. Ding, Y. Hu, T. Wang, and S. Yang, IEEE Trans. Energy Convers. **32**, 382 (2017).
[5] S. G. Oh and R. Krishnan, IEEE Trans. Ind. Appl. **43**, 1247 (2007).
[6] S. Prabhu, M. Balaji, and V. Kamaraj, in Proceedings of IEEE 11th International Conference on Power Electronics and Drive Systems, Sydney, NSW (2015).
[7] H. Hayashi, K. Nakamura, A. Chiba, T. Fukao, K. Tungpimolrut, and D. Dorrell, IEEE Trans. Energy Convers. **24**, 819 (2009).
[8] J. Kartigeyan and M. Ramaswamy, J. Magn. **22**, 93 (2017).
[9] Prabhu Sundaramoorthy and Balaji Mahadevan, J. Magn. **23**, 350 (2018).
[10] R. Arumugam, J. F. Lindsay, and R. Krishnan, Inernational Conf. Rec. IEEE IAS Annu. Meeting, Pittsburgh, PA, **1**, 50 (1988).
[11] M. Balaji, S. Ramkumar, and V. Kamaraj, J. Electr. Eng. Technol. **9**, 136 (2014).
[12] M. Moallem, C.-M. Ong, and L. E. Unnewehr, IEEE Trans. Ind. Appl. **28**, 364 (1992).
[13] C. Neagoe, A. Foggia, and R. Krishnan, IEEE International Conference on Electric Machines and Drives (1997).
[14] Y. K. Choi, H. S. Yoon, and C. S. Koh, IEEE Trans. Magn. **43**, 1797 (2007).
[15] N. K. Sheth and K. R. Rajagopal, IEEE Trans. Magn. **40**, 2035 (2004).
[16] M. Augustine, M. Balaji, and V. Kamaraj, in Proceedings of International Conference on Energy, Systems and Information Processing (ICESIP), India (2019).
[17] W. Ding, H. Fu, and Y. Hu, IEEE Trans. Power Syst. **33**, 482 (2018).
[18] K. N. Srinivas and R. Arumugam, IEEE Trans. Magn. **40**, 1911 (2004).
[19] Md Ashfanoor Kabir and Iqbal Hussain, in Proceedings of IEEE Energy Conversion Congress and Exposition (ECCE), Milwaukee, WI, USA (2016).
[20] Yudai Matsuo, Tsuyoshi Higuchi, Takashi Abe, Yasuhiro Miyamoto, and Motomichi Oht, in Proceedings of International Conference on Electrical Machines and Systems, Beijing, China (2011).
[21] J. Oyama, T. Higuchi, T. Abe, and K. Tanaka, J. Electr. Eng. Technol. **1**, 58 (2006).
[22] V. Ramanarayanan, L. Venkatesha, and Debiprasad Panda, in Proceedings of International Conference on Power Electronics, Drives and Energy Systems for Industrial Growth, New Delhi), India (2002).